

SURFACE-MICROMACHINED MILLIMETER-WAVE ANTENNAS

Yong-Kyu Yoon, Bo Pan, John Papapolymerou, Manos Tentzeris, and Mark G. Allen

School of Electrical and Computer Engineering
Georgia Institute of Technology, Atlanta, GA 30332, USA
Email: yongkyu.yoon@ece.gatech.edu

ABSTRACT

This paper reports various three-dimensional (3-D) surface micromachining technologies and their successful application to a variety of millimeter-wave antennas. Contrary to conventional planar type printed-circuit antenna structures, the 3-D surface micromachined structures described here minimize substrate effects, enabling substrate independence, high electrical performance, and broad bandwidth. The key technologies exploited include epoxy-core conductor technology, magnetic assembly, and electroplating bonding technology. Four millimeter-wave vehicles illustrate the technology: a monopole-driven Yagi-Uda (M-Yagi) antenna; an air-lifted patch antenna; an air-lifted coupler; and an air-lifted monopole antenna.

Key words: monopole-driven Yagi-Uda antenna, air-lifted patch antenna, air-lifted coupler, air-lifted monopole antenna, epoxy-core conductor, electroplating bonding, magnetic assembly

INTRODUCTION

Millimeter-wave devices are highly valued for their ability to provide very-broad-bandwidth wireless communication in both space and terrestrial applications. Examples include satellite, radar, mobile collision detection, imaging, and indoor local communications [1, 2]. One of the key components for a wireless millimeter wave system is its antenna. Currently, planar millimeter-wave antennas such as microstrip antennas or printed-circuit patch antennas are widely used due to their ease of manufacture, low cost, simple fabrication, and relative ease of integration with monolithic systems. However, those printed-circuit antennas can suffer from relatively narrow bandwidth, substrate dielectric loss, mutual coupling with their substrate, and surface wave perturbation issues [3]. An air-lifted 3-D antenna approach can be considered as an alternative to a printed-circuit antenna approach, with concomitant advantages of broad bandwidth, low loss, and reduced dependence on substrate. However, the fabrication difficulty associated with such 3-D structures has heretofore prevented them from being efficiently implemented in a cost effective, integrated fashion.

The characteristic size of electromagnetic antennas is determined by operation frequency; for millimeter-waves (30 GHz ~ 300 GHz), quarter-wave length scales range from 0.25mm to 2.5 mm. Recent advances in 3-D MEMS fabrication enable structures of this scale to be implemented in all three dimensions. Advanced surface-micromachined 3-D MEMS technologies include an epoxy-core conductor

technology [4-6], magnetic-force-driven actuating or assembly [7-10], self-assembly using surface tension [11], an electroplating bonding technology [12], and a plate-through-via-mold technology [13].

In this paper, exploiting the key technologies of epoxy-core conductors, magnetic assembly, and electroplating bonding, four millimeter-wave structures are fabricated and characterized: a monopole-driven Yagi-Uda (M-Yagi) antenna, an air-lifted patch antenna, an air-lifted coupler, and an air-lifted monopole antenna.

MONOPOLE-DRIVEN YAGI-UDA ANTENNA

A 3-D W-band surface micromachined monopole antenna has been reported using epoxy-core conductor technology [5,6]. It demonstrated desirable broad bandwidth (76-95 GHz) and low-loss performance. The monopole antenna inherently possesses the property of omni-directional radiation. In certain applications requiring high directivity, such as local chip communication or directional radiation with a low power budget, the omni-directional monopole antenna is not appropriate, but a monopole array providing more directivity will be necessary. By placing various parasitic monopoles on the ground plane nearby the driving poles, directivity will be increased in the same manner as the conventional dipole-driven Yagi-Uda antenna with directors and reflectors placed in proximity to the driving dipole. With the help of the ground as a mirror plane, a monopole-driven vertical Yagi-Uda antenna, the so-called M-Yagi antenna, can be implemented as shown in Figure 1. It consists of one driving monopole, one reflector, and several directors. The coplanar waveguide (CPW) feed is connected to the driving monopole.

This architecture provides several benefits: high radiation efficiency with minimum substrate effects due to an air-extruded architecture, easy and simple connectivity using a CPW-fed monopole with no need of complicated matching baluns or transformers, and a low-temperature

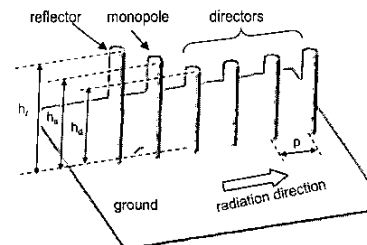


Figure 1. A monopole driven vertical Yagi-Uda antenna (M-Yagi) architecture.

TRANSDUCERS'05

The 13th International Conference on Solid-State Sensors, Actuators and Microsystems, Seoul, Korea, June 5-9, 2005

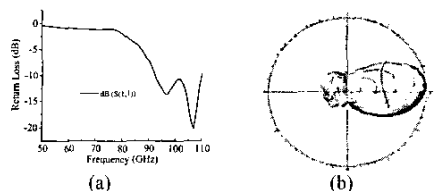


Figure 2. Simulated performance of 5-element array: (a) Return loss, (b) Top view radiation pattern at 95 GHz.

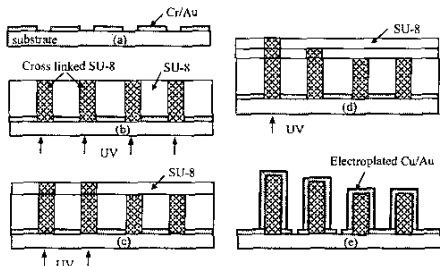


Figure 3. Fabrication process of an M-Yagi antenna.

CMOS compatible fabrication process allowing the potential for ease of integration on other RF chips in a post-processing fashion.

Full-wave electromagnetic simulations have been performed using the Ansoft high frequency structure simulator (HFSS) 9.1. The spacing between adjacent elements is set to 480 μm . The height for reflector, driving monopole, and directors are 800 μm , 715 μm , 560 μm , respectively. The predicted return loss and radiation pattern for a 5-element Yagi-Uda antenna are plotted in Figures 2a and 2b, respectively. The simulated radiation pattern gives a maximal directivity of 8.2 dBi in the horizontal axis.

High-aspect-ratio surface micromachining technology is the key enabling technology for this structure. Figure 3 shows the fabrication process for the M-Yagi antenna. Three layers of photopatternable epoxy SU-8 (Microchem, Inc.) are spin coated and photopatterned on a chromium patterned glass substrate in a sequential fashion to define



Figure 4. Photomicrograph of a fabricated 5-element M-Yagi antenna.

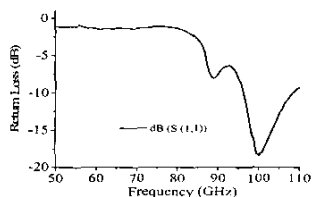


Figure 5. Measured return loss between 50-110 GHz.

the height of the directors, the driving monopole, and the reflector, respectively (Figure 3abcd). Metal coated epoxy poles are fabricated (Figure 3e) using proximity lithography as in [4-6]. Figure 4 shows a fabricated 5-element M-Yagi with a 700 μm tall monopole as the driving monopole.

The fabricated antenna was characterized using an Agilent 8510XF network analyzer and Cascade ACP 110 probes with 150 μm pitch. The NIST Multical TRL algorithm [14] was used to calibrate the measurement system. Figure 5 shows the measured return loss between 50 GHz and 110 GHz for a 5-element M-Yagi antenna. It shows a radiation resonance at approximately 100GHz with a return loss of 18 dB, demonstrating a good agreement with the simulated results. 12 % of a very wide 10-dB-bandwidth has been achieved. The radiation measurement is under investigation.

AIR-LIFTED PATCH ANTENNA

Figure 6 shows a monopole-driven air-lifted patch antenna for Ka-band (20GHz-30GHz) application. The patch is supported by a metal coated epoxy-core monopole as well as structural polymer (SU-8) supporting posts, in contrast to the all metal posts in [13]. Lifting the patch from the substrate improves its substrate-related loss and bandwidth.

The elevated patch antenna is fabricated by a combination of the epoxy-core conductor technique [5], laser machining, and electroplating bonding [6]. Figure 7 illustrates the key fabrication steps. After a high aspect ratio 600 μm tall SU-8 is patterned using UV photolithography, a feeding monopole is selectively metallized using photolithography and electrodeposition to provide a signal path from a coplanar waveguide (CPW) to the patch (Figure 7 upper). The metal patch is separately fabricated from a copper sheet with a thickness of 100 μm by laser ablation. After adhering the patch to the posts using conductive paste,

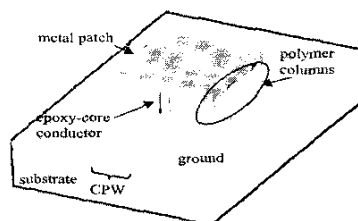


Figure 6. Air-lifted patch antenna.

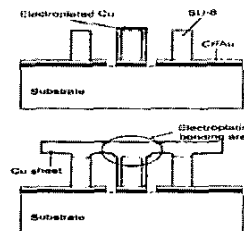


Figure 7. Fabrication process of an air-lifted patch antenna.

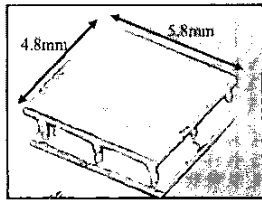


Figure 8. Photomicrograph of a fabricated air-lifted patch antenna.

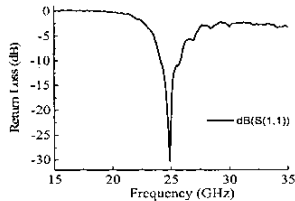


Figure 9. Measured return loss of an air-lifted patch antenna.

additional copper electroplating bonding between the feeding monopole and the patch is performed up to a thickness of 30 μm to strengthen the connection (Figure 7 lower).

The fabricated air-lifted patch antenna (Figure 8) has been characterized between 10 GHz and 50 GHz. The patch is 4.8 mm x 5.8 mm in size and the measurement result shows a resonant frequency of 25 GHz with a return loss of 30 dB for the fabricated patch antenna as shown in Figure 9. The frequency is slightly shifted from the design and this shift is attributed to the small geometry disparity between the fabricated prototype and the simulated one. A 10 dB bandwidth of 7 %, from 24.1 GHz to 25.8 GHz, has been measured. This compares favorably to conventional printed patch antenna bandwidths of 1~5%, which are limited in part due to the effects of the substrate.

AIR-LIFTED COUPLER

Figure 10 shows a broadband air-lifted microstrip coupler, where the coupler is elevated to a height of several hundred micrometers from the substrate [15]. Two parallel bridges are air-coupled and fed by a combination of epoxy-core metal posts and CPW. Since the substrate is covered by a ground plane except for the coplanar waveguide, electromagnetic coupling with the substrate is reduced. Also, the elimination of the dielectric/air interface around the coupler helps to reduce the mode dispersion and associated problems such as poor isolation. Therefore, this scheme can be considered as a unique method to develop

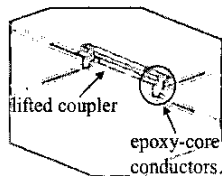


Figure 10. Air-lifted coupler.

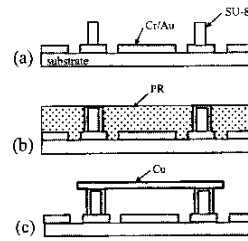


Figure 11. Fabrication process of an air-lifted coupler.

high performance RF front-end components on lossy substrates.

The fabrication of the coupler is detailed in Figure 11. The CPW and the ground planes are patterned using chromium and gold (Cr / Au; 30 nm / 1.5 μm) on top of a soda-lime glass substrate with dielectric constant ϵ_r of 7.75 by means of a standard lift-off process. SU-8 is spin-cast and patterned for the post definition to the desired height. In this coupler implementation, feeding posts have a height of 190 μm (11a). Conformal seed layers of titanium and copper (Ti / Cu; 30 nm / 300 nm) have been deposited using a DC sputterer. Negative-tone photo resist NR9-8000 (Futurrex, Inc.) is spin-coated and lithographically patterned, letting copper selectively cover the posts with a thickness of 15 μm . A thick sacrificial polymer (NR9-8000) has been used as a mechanical support for the subsequent bridge patterning (11b). Seed layers of Ti / Cu for the bridge patterning are deposited, followed by photoresist (NR9-8000) casting and patterning on it. After copper electrodeposition with a thickness of 10 μm , removal of molding polymer, seed layers, and sacrificial layers are performed to complete the process (11c).

Figure 12 shows a fabricated air-lifted coupler with 190 μm air gap between the coupler and the ground substrate. After TRL calibration as before, four port RF characteristics have been performed as shown in Figure 13. The coupler demonstrates a broadband coupling of 12.5 dB and a matching better than 10 dB over 15-45 GHz. It also shows a through transmission of 0.015-1.85 dB over 15-45 GHz.

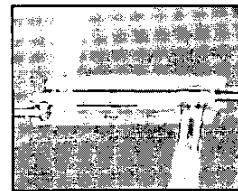


Figure 12. Photomicrograph of a fabricated air-lifted coupler.

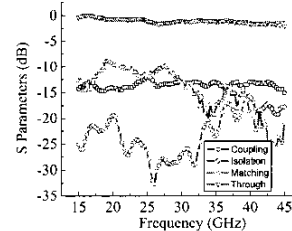


Figure 13. Measured performance of an air-lifted coupler.

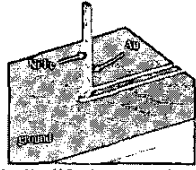


Figure 14. Magnetically-lifted monopole antenna.

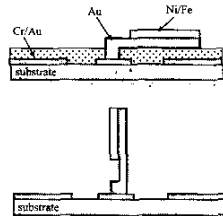


Figure 15. Fabrication process of a magnetically-lifted monopole antenna.

MAGNETICALLY-LIFTED MONOPOLE ANTENNA

Figure 14 shows a magnetically lifted monopole antenna. The antenna consists of soft metal (gold) for plastic deformation during bending [8], and a ferromagnetic metal (NiFe) for the magnetic-force-based deflection [7-10]. A cantilever is fabricated using PR mold patterning and electrodeposition processes (Figure 15 upper). After the cantilever is released, it is erected vertically using an external magnetic field. The erected structure stays in the vertical position after plastic deformation of the gold layer (Figure 15 lower). Figure 16 shows a fabricated magnetically-lifted structure. The cantilever has a width of $80\ \mu\text{m}$ and a length of 2 mm. The thicknesses of the gold layer and the ferromagnetic layer are $5\ \mu\text{m}$ and $6\ \mu\text{m}$, respectively. The air-lifted structure shows a monopole antenna performance in far-field radiation. A return loss of 24 dB at 35 GHz with a bandwidth of 20.7 % is shown in Figure 17.

CONCLUSIONS

Four surface-micromachined millimeter-wave structures, a monopole-driven Yagi-Uda antenna; an air-lifted patch antenna; an air-lifted coupler; a magnetically-lifted monopole antenna, have been fabricated using advanced 3-D MEMS technologies including an epoxy-core technology, magnetic assembly, and an electroplating bonding technology. Also their RF characterizations have been performed. Very broad bandwidths of 7 ~ 21% have been achieved with those air lifted structures. Each of those devices shows record performance for micromachined antennas.

REFERENCES

[1] F.K. Schwering, "Millimeter Wave Antennas," *Proceedings of the IEEE*, vol. 80, no. 1, pp. 92-102, January, 1992.

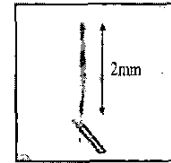


Figure 16. Fabricated magnetically-lifted monopole antenna.

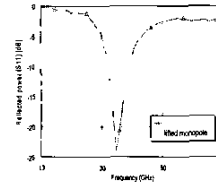


Figure 17. Measured return loss of a fabricated magnetically-lifted monopole antenna.

- [2] G.M. Rebeiz, "Millimeter-Wave and Terahertz Integrated Circuit Antennas," *Proceedings of the IEEE*, vol. 80, no. 11, pp. 1748-1770, November, 1992.
- [3] D.M. Pozar, "Considerations for Millimeter Wave Printed Antennas," *IEEE Trans. Antennas and Propagation*, vol. AP-31, no. 5, pp. 740-747, September, 1983.
- [4] Y.-K. Yoon, J.-W. Park, and M.G. Allen, "RF MEMS Based on Epoxy-Core Conductors," *Solid-State Sensor, Actuator, and Microsystems Workshop*, Hilton Head Island, SC, USA, pp. 374-375, 2002.
- [5] Y.-K. Yoon, B. Pan, P. Kirby, J. Papapolymerou, M. Tentzeris, and M.G. Allen, "Surface Micromachined Electromagnetically Radiating RF MEMS," *Solid-State Sensor, Actuator, and Microsystems Workshop*, Hilton Head Island, SC, USA, pp. 328-331, 2004.
- [6] B. Pan, Y.-K. Yoon, P. Kirby, J. Papapolymerou, M. Tentzeris, and M.G. Allen, "A W-band Surface Micromachined Monopole for Low-cost Wireless Communication Systems," *IEEE International Microwave Symposium*, Fort Worth, TX, USA, pp.1935-1938, June, 2004.
- [7] W.P. Taylor, O. Brand, and M.G. Allen, "Fully integrated magnetically actuated micromachined relays," *J.MEMS*, vol. 7, no. 2, pp. 181-191, 1998.
- [8] J. Zou, J. Chen, Ch. Liu, and J.E. Schutt-Aine, "Plastic deformation magnetic assembly of out of plane microstructures: technology and application," *J. MEMS*, vol. 10, no. 2, pp. 302-309, 2001.
- [9] Y. Choi, K. Kim, and M.G. Allen, "A Magnetically Actuated, Electrostatically Clamped High Current MEMS Switch," *ASME IMECE*, New York, NY, USA, Nov. 2001.
- [10] I.-J. Cho, T. Song, S.-H. Baek, and E. Yoon, "A Low-Voltage Push-Pull SPDT RF MEMS Switch Operated by Combination of Electromagnetic Actuation and Electrostatic Hold," *IEEE MEMS*, Miami, FL, USA, pp. 32-35, 2005.
- [11] G.W. Dahmann, E.M. Yeatman, P. Young, I.D. Robertson, and S. Lucyszyn, "High Q Achieved in Microwave Inductors Fabricated by Parallel Self-Assembly," *International Conference on Solid-State Sensors and Actuators*, Munich, Germany, June 10-14, 2001, pp. 1098-1101.
- [12] Y.-H. Joung, S. Nuttinck, S.-W. Yoon, M.G. Allen, and J. Laskar, "Integrated inductors in the chip-to-board interconnect layer fabricated using solderless electroplating bonding," *IEEE International Microwave Symposium*, Seattle, WA, USA, pp.1409-1412, 2002.
- [13] M.-L. Ha, Y.-H. Cho, C.-S. Pyo, and Y.-S. Kwon, "Q-band Micro Patch Antennas Implemented on a High Resistivity Silicon Substrate Using the Surface Micromachining Technology," *IEEE International Microwave Symposium*, Fort Worth, TX, USA, pp.1189-1192, 2004.
- [14] R.B. Marks, "A multiline method of network analyzer calibration," *IEEE Trans. MTT*, vol. 39, no.12, pp. 1205-1215, Dec. 1991.
- [15] B. Pan, Y.-K. Yoon, Y. Zhao, J. Papapolymerou, M. Tentzeris, M.G. Allen, "A Broadband Surface-Micromachined 15-45 GHz Microstrip Coupler," will be presented in *IEEE International Microwave Symposium*, Long Beach, CA, USA, June 12-17, 2005